TEXTURIZATION OF MONOCRYSTALLINE SILICON BY METAL-ASSISTED CHEMICAL ETCHING: ANALYSIS OF REACTION DYNAMICS

David Pera, Ivo Costa, Filipe Serra, Afonso Guerra, Killian Lobato, João M. Serra, José A. Silva
Instituto Dom Luiz - Faculdade de Ciências Universidade de Lisboa
Edifício C1, Campo Grande, 1749-016 Lisboa, Portugal

ABSTRACT: We present here recent results of an optimized metal-assisted chemical etching (MACE) based process. The process consists of a simple maskless etching based on the use of a solution of hydrogen peroxide (H_2O_2), hydrofluoric acid (HF), and silver nitrate ($AgNO_3$). H_2O_2 and HF work as etching agents, while $AgNO_3$ donates silver ions that locally catalyze the etching reaction, creating steep and anisotropic structures on the surface and sharply reducing its reflectivity. In this study Czochralski monocrystalline silicon wafers both p-type and n-type were used as substrates and the etching time was swept between 30 s and 270 s. It was observed that, although for optimal conditions p-type and n-type wafers achieved similar reflectance values after etching, the reaction's dynamic showed to be dependent on the doping type and concentration level (resistivity). The lowest effective reflectivity (R_{eff}) reached during this study was 3.0%, obtained for a p-type wafer.
Keywords: Crystalline, silicon, texturization, light-trapping

1 INTRODUCTION

Improving the efficiency of photovoltaic systems is a goal increasingly pursued by the photovoltaic industry. One of the most effective ways to improve the efficiency of photovoltaic cells and systems is by increasing the number of photons that reach and are absorbed in the solar cell active area, thus boosting the solar cell photocurrent. Also, by enhancing the solar cells' light-capture efficiency, thinner and lower quality substrates can be used, allowing significant reductions in the device's production costs [1].

The standard method to reduce front surface reflectivity in crystalline silicon solar cells is to perform a chemical etching with an alkaline or acidic bath, followed by the deposition of a hydrogenated silicon nitride film by PECVD [2]. In the last years, several innovative strategies to improve light capture in solar cells have been proposed, such as the use of plasmonic structures [3]. However even if the introduction of plasmonic structures can produce a significant increase absorption, for certain regions of the electromagnetic spectrum, the overall light absorption gain, averaged in the AM1.5 spectrum, is not weighty. The use of reactive ion etching (RIE) to produce nanostructures that enhance solar cells light-capture is seen as very promising approach [4]. But until know a cost-efficient RIE based process, to be used in industrial solar cell production has not been demonstrated. The interest in the use of metal-assisted chemical etching (MACE) [5] based methods to reduce the reflectivity of the solar cells' front surface has increased significantly in the last years. Due to its simplicity, scalability, and potential cost-effectiveness, MACE is one of the most promising light-trapping techniques to be applied in the industrial production of high-efficiency crystalline silicon solar cells. In fact, the capability of this technique to increase the solar cell efficiency has already been demonstrated [6].

In our study we use a simple maskless MACE process based on the use of a solution of hydrogen peroxide (H_2O_2), hydrofluoric acid (HF), and silver nitrate ($AgNO_3$). The process has been characterized and optimized in previous studies [7,8]. Here we analyze the reaction dynamics and compare results for p-type and n-type silicon.

2 METHODS

2.1 Etching process

The mechanics of the MACE texturization process is well known [7], the substrates are dipped in the etching solution. H_2O_2 acts as oxidation agent while HF removes the silicon oxide formed, according to the equation:

$$\mathrm{Si} + H_2O_2 + 6HF \rightarrow 2H_2O + H_2SiF_6 + H_2 \qquad (1)$$

$AgNO_3$ is dissociated in the solution, donating holes to the reaction thus catalyzing it. Consequently, the presence of silver originates faster etching reactions and deeper texturizations.

During this study three groups of Czochralski monocrystalline silicon wafers were used: (i) 1-3 Ω.cm p-type (boron doped); (ii) 10-20 Ω.cm p-type (boron doped); (iii) n-type (phosphorous doped) 3-7 Ω.cm. For all these wafers the surface orientation was (100).

During this study the concentrations of the three reactants were fixed (Table I) and the etching time was varied between 30 and 270 seconds.

Table I: Reactants' concentrations used

	Concentration (mol/l)
HF	12
H_2O_2	1.1
$AgNO_3$	6×10^{-3}

Since the etching reaction is highly exothermic and the reaction's kinetics is strongly dependent on the temperature. To adequately characterize the reaction's dynamics, controlling the reaction temperature is mandatory. For this purpose, the reaction beaker was placed in a water buffer bath kept at 30˚C and the evolution of the reactants' temperature was carefully monitored. After removal from the etching bath, the wafers were rinsed in deionized water. To remove the silver deposit, the wafers were then dipped in a nitric acid solution, and again rinsed in deionized water.

2.2 Characterization

To analyze the mass variation during the MACE process, the wafers' mass was measured before etching and after silver removal. The spectral reflectance of the etched surfaces was measured in the range 350-1100 nm with an UV-vis Spectrophotometer Shimadzu UV – 2600 PC. The effective reflectivity R_{eff} was calculated by weighting the reflectance values with the reference AM1.5 spectrum [9] according to equation (2), where R_λ and n_λ are respectively the reflectance measured and the number of photons in the AM1.5 spectrum for the wavelength λ.

$$R_{\text{eff}} = \frac{\sum_\lambda R_\lambda n_\lambda}{\sum_\lambda n_\lambda} \qquad (2)$$

Moreover, the structural characterization of the textured surfaces was carried out through scan electron microscope (SEM) observations.

3 RESULTS

3.1 Structural characterization

In Figure 1 a SEM crosscut image of a MACE etched p-type silicon wafer is presented. The disordered nature of the nanostructures created is noticeable, also the typical height of the nanostructures can be estimated to be around 2 nm. The observations made on n-type silicon wafers etched in analogous conditions, showed similar surface morphology.

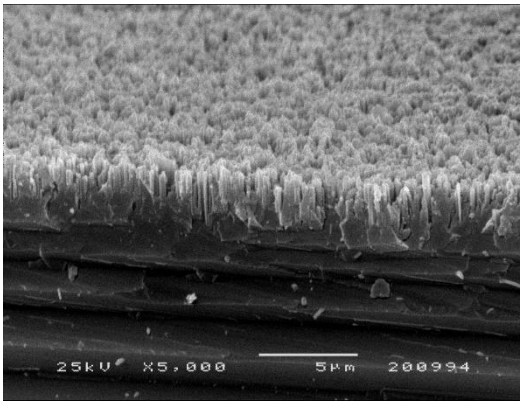

Figure 1: SEM image of p-type silicon wafer, 1-3 Ω.cm etched during 120 s.

3.2 Mass variation

The variation of the wafers' mass during etching is presented in Figure 2. It can be observed that for the three groups of wafers texturized, the mass is linearly reduced with the etching time.

We can also observe that, for the etching times tested, the reduction of mass over time is very similar for the samples type n (3-7 Ω.cm), and type p II (10-20 Ω.cm).

When comparing the mass reduction for wafers p-type I (1-3 Ω.cm) with the remaining groups we can conclude that the mass reduction rate is slightly lower. In fact, for p-type I wafers the Δm/m (t) line slope is $m=1.6\times10^{-3}$, compared to 1.8×10^{-3} for the other two series of wafers. The results suggest that for n- and p-type wafers with comparable resistivities, the etch rate is approximately 10% higher for n-type ones. It must be mentioned that such difference in the reaction dynamics, for the two types of silicon, is lower than the values previously reported in the literature for MACE based processes [10].

On the other hand, the results obtained for p-type wafers with different levels of resistivity, suggest etching rate increases with the doping level, agreeing with previous results [10].

Finally, it is clear that for the p-type I wafers' group, the mass reduction as function of time is significantly delayed nearly 30 s when for the two-remaining wafers' groups (i.e., the series is shifted to the left). Such result might be attributed to a different initial surface condition for the wafers comprised in this group.

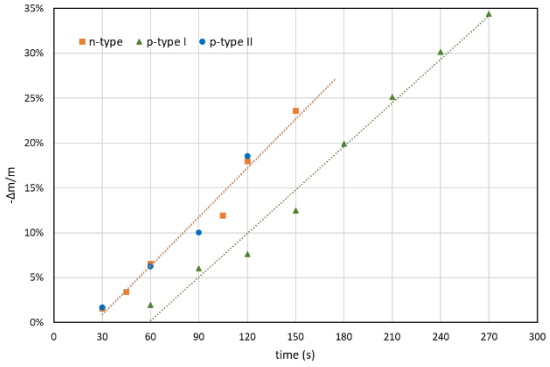

Figure 2: Mass variation as function of etching time for silicon wafers n-type (3-7 Ω.cm), p-type I (ρ ~ 1-3 Ω.cm) and p-type II (ρ ~ 10-20 Ω.cm).

3.2 Reflectance

In Figure 3 the reflectance curves after the etching process, for a n-type and a p-type wafer are compared. The reference spectrum AM1.5 is also presented (secondary axis). It can be observed that for the most spectral range the reflectance is very similar for both wafers. The only noticeable differences are observed in the ultraviolet and near-infrared regions, where the n-type wafer slightly higher reflectance values. It must be mentioned that such differences are inside the typical variability of the reflectance measurement process and were not considered significant.

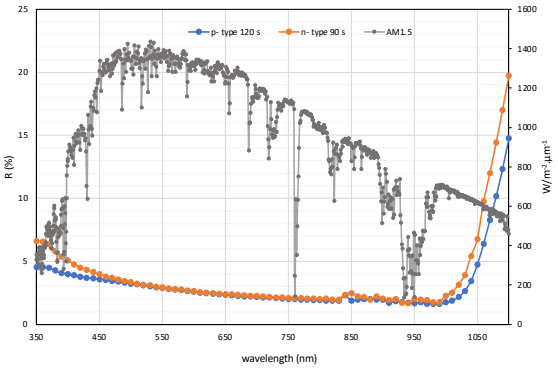

Figure 3: Reflectance curves for a p-type wafer (ρ ~ 1-3 Ω.cm) and n-type wafer (3-7 Ω.cm), in the range 350-1100 nm.

Based on the reflectance curves obtained and using equation (2) the R_{eff} values were obtained. The lowest R_{eff} obtained for n-type wafers was R_{eff}=3.0%, while for n-type the minimum was R_{eff}=3.3%.

4 CONCLUSIONS

The aim of the study here presented was to analyze sensibility of the reaction dynamics of a MACE based process, on doping type and concentration, by performing etchings of n- and p-type wafers with several etching times.

It was observed that the mass removal rates were similar for the three groups of samples, showing a linear behavior of the MACE process. For the same etching conditions and similar resistivities mass removal in n-type samples showed to be slightly faster than for p-type wafers. When comparing p-type samples with resistivity values with one order of magnitude difference, results showed that the mass removal increases for higher resistivity.

The reflectance measurements showed no significant difference between the three sets of samples. The lowest R_{eff} obtained for p-type was 3.0% while for n-type was 3.3%.

5 REFERENCES

[1] Y. Liu, W. Zi, S. Liu, and B. Yan, 'Effective light trapping by hybrid nanostructure for crystalline silicon solar cells', Solar Energy Materials and Solar Cells 140 (2015) 180-186.

[2] S. W. Glunz, R. Preu, and D. Biro. 'Crystalline silicon solar cells: state-of-the-art and future developments', Comprehensive Renewable Energy 1 (2012) 353-387.

[3] F. Enrichi, A. Quandt and G. C. Righini, 'Plasmonic enhanced solar cells: Summary of possible strategies and recent results', Renewable and Sustainable Energy Reviews 82 (2018) 2433-2439.

[4] H. S. Lee, J. Suk, H. Kim et al., 'Enhanced efficiency of crystalline Si solar cells based on kerfless-thin wafers with nanohole arrays', Science Reports 8 (2018) 3504.

[5] K. Tsujino, M. Matsumura and Y. Nishimoto, 'Texturization of multicrystalline silicon wafers for solar cells by chemical treatment using metallic catalyst', Solar Energy Materials and Solar Cells 90 (2006) 100-110.

[6] J. Oh, H.C. Yuan, H.M. Branz, 'An 18.2%-efficient black-silicon solar cell achieved through control of carrier recombination in nanostructures', Nature Nanotechnology 7 (2012) 743-748.

[7] I. Costa, D. Pera, J. A. Silva, 'Improving light capture on crystalline silicon wafers', Materials Letters 272 (2020) 127825.

[8] D. Pera, et al. 'Advanced light-trapping structures for back-contact solar cells produced by metal-assisted chemical etching.' Proceedings 37th European Photovoltaic Solar Energy Conference (2020) 354 - 357.

[9] ASTM, 'Reference Solar Spectral Irradiance: Air Mass 1.5', American Society for Testing and Materials (ASTM) Terrestrial Reference Spectra for Photovoltaic Performance Evaluation, 2003. [Online]. Available: http://rredc.nrel.gov/solar/spectra/am1.5/.

[10] Z. Huang, N. Geyer, P. Werner, J. De Boor, and U. Gösele, 'Metal-assisted chemical etching of silicon: A review', Advanced Materials. 23.2 (2011) 285-308.

6 AKNOWLEDGEMENTS

The authors acknowledge the financial support of the Portuguese Fundação para a Ciência e Tecnologia (FCT) through the projects TaCIt / PTDC/NAN-OPT / 28837 / 2017 and UIDB / 50019 / 2020 – IDL.

We would also like to thank Dr. Olinda Monteiro for the use of the UV-Vis Spectrophotometer and Telmo Nunes for performing the scan electron microscope observations.